International Journal of Solids and Structures 69–70 (2015) 189–194

Contents lists available at ScienceDirect

International Journal of Solids and Structures

journal homepage: www.elsevier.com/locate/ijsolstr

Adhesion of a gas-filled membrane on a stretched substrate

Lei Chen, Shaohua Chen *

LNM, Institute of Mechanics, Chinese Academy of Sciences, Beijing 100190, China

ARTICLE INFO

Article history:
Received 25 January 2015
Received in revised form 19 April 2015
Available online 10 June 2015

Keywords:
Adhesive contact
Gas-filled membrane
Stretched substrate
Free energy
Cell adhesion

ABSTRACT

A two-dimensionally adhesive contact model is established, in which a gas-filled elastic membrane adheres on a stretched substrate. The free energy of the system is achieved, minimization of which leads to the relationship between the contact width and the global substrate strain. The contact solution exhibits three distinct regimes characterized by two threshold strains: (i) the contact size is hardly affected by the external loading acted on the substrate when the global substrate strain is below the first threshold value; (ii) the size of the contact is reduced quickly as the force is between the two threshold levels; (iii) the contact size tends to vanish when the global substrate strain exceeds the second threshold level. All the results share a number of common features with the experimental observation of cell orientation on a stretched substrate. Effects of the internal pressure, the tensile stiffness of the membrane and the interface work of adhesion on the two threshold levels are further discussed. The finding in the present paper should be helpful for deep understanding of adhesion mediated deformation sensing mechanism by which cells can detect mechanical signals in extracellular matrices and the design of adhesion mediated deformation sensors.

1. Introduction

Adhesion among different types of cells and between cells and substrates is of great interest in many fields of biology, including embryonic development, cancer metastasis, cellular transport, endo- and exocytosis, tissue and cellular engineering (Alberts et al., 1994; Bao and Suresh, 2003; Gao et al., 2005). Mechanical signals are believed to play an important role in cell adhesion. For example, cells are known to respond to mechanical forces exerted by the surrounding fluid, adhering beads or substrates (Choquet et al., 1997; Girard and Nerem, 1995; Ingber, 1993; Wang et al., 1993), they could detach, slip or roll on a substrate in response to these forces (Bischofs and Schwarz, 2003; Galbraith and Sheetz, 1998; Geiger and Bershadsky, 2002; Haston et al., 1983; Huang and Ingber, 1999; Lorz et al., 2000; Wong et al., 2003). Furthermore, cells could sense the stiffness gradient of substrates and migrate towards the stiffer segment (Lo et al., 2000). Even for oosperm transport from ovary to uterus, the behavior of smooth muscle contraction is much essential, which could induce a moving strain gradient field as a driving force for oosperms' rolling. A recently biomimetic experiment further suggests that an elastic strain gradient in substrates can be utilized to transport spherical particles on a stretchable substrate by rolling (Chen et al., 2014).

Another set of experiments have shown that cells cultured on a cyclically stretched substrate tend to reorient themselves away from the stretch direction (Buck, 1980; Dartsch and Hammerle, 1986; Jungbauer et al., 2008; Moretti et al., 2004; Neidlingerwilke et al., 1994; Wang et al., 1995). Dartsch and Hammerle (1986) further noted that cells did not respond to small stretch amplitudes (less than 2%), suggesting that there exists a threshold stretch amplitude to initiate cell reorientation. Above this threshold, an increasing number of cells begin to respond to substrate deformation by reorienting themselves away from the stretch direction. The larger the stretch amplitude, the more cells reorient. Almost all cells join the reorientation process once the stretch amplitude exceeds a second threshold level about 5–6% (Neidlingerwilke et al., 1994).

How could cells sense the substrate deformation? An adhesive contact model (Chen and Gao, 2006b) was established in order to explain cells reorientation from the mechanics point of view, in which an elastic solid cylinder was used and the contact interface was treated as a well-bonded region without slippage to simulate tremendously focal adhesion between cells and substrates. Theoretical predictions agree well with experimental observations, especially the two threshold strains controlling the process of cell reorientation. Non-slipping adhesive contact model between two dissimilar solid spheres subjected to a pair of pulling forces and a mismatch strain suggests an adhesion mediated deformation sensing mechanism by which cells and molecules can detect mechanical signals in the environment via adhesive interactions (Chen and Gao,

* Corresponding author. Tel.: +86 10 82543960; fax: +86 10 82543977.
E-mail address: chenshaohua72@hotmail.com (S. Chen).

http://dx.doi.org/10.1016/j.ijsolstr.2015.04.037
0020-7683/

2006a). In microscopic views, cell–cell and cell-substrate adhesion was studied with statistical physics method, such as the well-known Bell's model (Bell, 1978). In order to interpret cell reorientation in experiments, Kong et al. (2008) established a stochastic model to investigate the stability of focal adhesion under a dynamic load by applying an externally cyclical strain on substrates, and found that a threshold of the external strain amplitude exists beyond which the adhesion cluster disrupts quickly. Combining the statistical physics and the elastic contact theory, series of theoretical models were proposed in order to characterize cell-substrate adhesion (Gao et al., 2011; Qian and Gao, 2010; Zhang et al., 2013, 2012), in which the effect of matrix stiffness (Qian and Gao, 2010), anisotropy of matrix material (Zhang et al., 2013), graded modulus of substrates (Zhang et al., 2012) and the pulling angle of external forces (Gao et al., 2011) were considered. Most of the researches treated cells as spherical membranes or capsules rather than elastic solids, which should be much closer to the real morphology of cells apparently (Hiramoto, 1963; Liu et al., 1996; Sen et al., 2005). Is there any difference between the model of an elastic solid and that of an elastic membrane in order to disclose the adhesion mediated deformation sensing mechanism of cells? Could a membrane model predict the two threshold levels for cell reorientation? What factors would influence the two values?

As for a spherical membrane in adhesion with a rigid substrate, several models have already been proposed and studied by Shanahan (1997, 2003), which was also adopted to investigate interactions between soft particles and substrates (Liu, 2006; Lulevich et al., 2004; Xu and Liechti, 2011). With the similar idea, a contact model of a gas-filled membrane adhering on a stretched substrate is first studied in the present paper. A liquid-filled membrane case will be considered in our future work though it looks more like a cell.

2. Theoretical model and analysis

A two-dimensionally adhesive contact model is shown in Fig. 1, which consists of three continuous stages: (i) the first one is called as a self-inflated stage, in which an elastic membrane of an intrinsic radius ρ and a tensile stiffness $E_m^* t_m$ is inflated by an internal pressure P_i, comparing to an environmental pressure P_0, in which $E_m^* = E_m$ is for a plane stress case and $E_m^* = E_m/(1-\nu_m^2)$ for a plane strain one, E_m and ν_m denote the Young's modulus and Poisson's ratio of the membrane, respectively. t_m is the membrane thickness with an assumption $t_m \ll \rho$. As a result, the additive gas pressure is $\Delta P_i = P_i - P_0$, which induces an inflated radius R_i and a tensile strain ε_i in the membrane. (ii) The second stage is addressed as a self-adhesion stage, in which the inflated membrane adhesively contacts an elastic substrate of length $2L$ and tensile stiffness $E_s^* t_s$, leading to a self-adhesion area of half-width a_a with a small contact central angle θ_a as shown in Fig. 1. Due to the self-adhesion, the internal pressure inside the membrane and the membrane radius change to be P_a and R_a, respectively. The tensile strain of the membrane changes from ε_i to ε_a, while the strain in the adhesion area remains to be ε_i due to an assumption of $E_s^* t_s \gg E_m^* t_m$ and a neglected deformation of the substrate in this stage. (iii) The last stage is called as a stretch stage, in which the elastic substrate is tensioned by an external force F, leading to a global substrate strain $\varepsilon_g = F/(E_s^* t_s)$. As a result, an updated adhesion width is $2a_F$ with a small contact central angle θ_F. The elastic membrane is further deformed, leading to an internal pressure P_F, radius R_F and membrane strain ε_F. Due to the assumption of a perfect adhesive interface between the membrane and the substrate, the adhesion part of the membrane will deform further along with the substrate.

Without loss of generality, we assume that the tensile stiffness of the membrane keeps unchanged in all three stages and the contact width is much smaller than the membrane radius, i.e. $a_a \ll R_a$ and $a_F \ll R_F$.

The quantity of internal gas is conservative, which abides by the ideal gas law, i.e.,

$$P_i V_i = P_a V_a = P_F V_F = n\tilde{R}\tilde{T} = K \text{ (constant)}, \tag{1}$$

where V_i, V_a and V_F denote volumes of the membrane in the first, second and last stages, respectively. n is the mole number of the gas contained, $\tilde{R}$ is the ideal gas constant and $\tilde{T}$ the absolute temperature with a constant $K = n\tilde{R}\tilde{T}$.

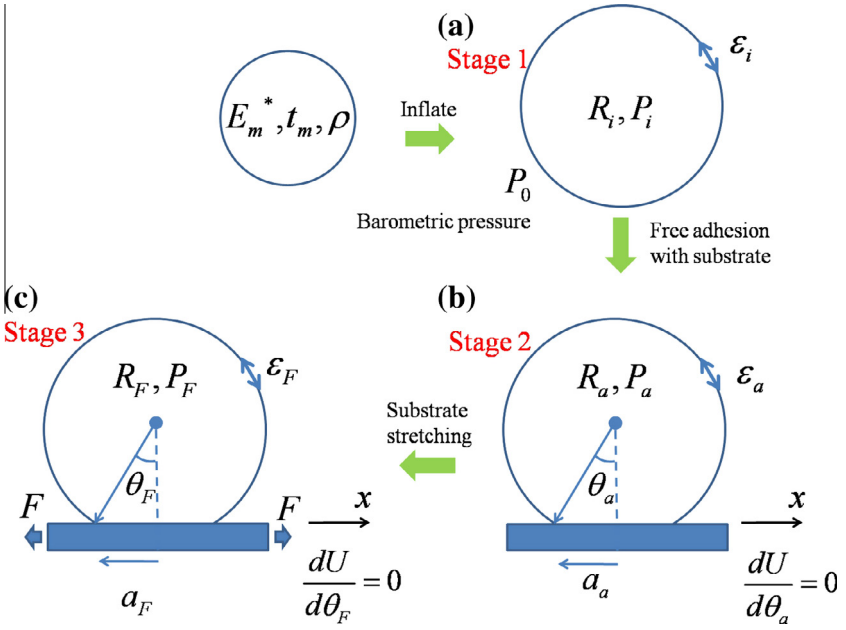

Fig. 1. The two-dimensionally adhesive contact model of an elastically gas-filled circular membrane on an elastic substrate and schematics of the included three stages, i.e., the self-inflated stage, the self-adhesion stage and the one subjected to an external loading on the substrate.

In the first stage. The tensile force within the membrane can be obtained according to a simple equilibrium as,

$$T_i = R_i \cdot \Delta P_i, \tag{2}$$

which leads to the tensile strain of the free membrane as

$$\varepsilon_i = \frac{R_i - \rho}{\rho} = \frac{T_i}{E_m^* t_m} = \frac{R_i \cdot \Delta P_i}{E_m^* t_m}. \tag{3}$$

In the second stage. Similar to the first stage, the tensile strain of the membrane outside the adhesion area after self-adhesion is

$$\varepsilon_a = \frac{R_a - \rho}{\rho} = \frac{T_a}{E_m^* t_m} = \frac{R_a \Delta P_a}{E_m^* t_m}, \tag{4}$$

where $\Delta P_a = P_a - P_0$.

Combining Eqs. (3) and (4) leads to the radius increment in the initial two stages,

$$\delta R_a = R_a - R_i = \frac{R_i^2 (P_a - P_i)}{E_m^* t_m - R_i (P_a - P_i)}. \tag{5}$$

The volume of the membrane per unit length after self-adhesion is given by

$$V_a \approx \pi R_a^2 \left(1 - \frac{2\theta_a^3}{3\pi}\right) \approx V_i \left(1 + \frac{2\delta R_a}{R_i}\right)\left(1 - \frac{2\theta_a^3}{3\pi}\right), \tag{6}$$

in which $V_i = \pi R_i^2$ is the volume per unit length in the first stage. Considering $P_i V_i = P_a V_a = K$ yields the internal pressure after self-adhesion,

$$P_a \approx P_i \left(1 - \frac{2\delta R_a}{R_i}\right)\left(1 + \frac{2\theta_a^3}{3\pi}\right). \tag{7}$$

Inserting Eq. (7) into (5) yields the radius increment in terms of θ_a

$$\delta R_a \approx \frac{2R_i^2 P_i \theta_a^3}{3\pi (E_m^* t_m + 2R_i P_i)} \equiv \lambda_i R_i \theta_a^3, \tag{8}$$

where we define $\lambda_i = \frac{2R_i P_i}{3\pi (E_m^* t_m + 2R_i P_i)}$.

Then, the radius R_a and the tensile strain ε_a of the elastic membrane can be written as

$$R_a = R_i + \delta R_a = (1 + \lambda_i \theta_a^3) R_i, \tag{9}$$

$$\varepsilon_a = \frac{R_a - \rho}{\rho} = \frac{(1 + \lambda_i \theta_a^3) R_i - \rho}{\rho}. \tag{10}$$

The free energy of the whole system U consists of the elastic strain energy stored in the membrane U_E, the interface adhesion energy U_S and the internal energy U_P induced by the compressive gas within the membrane, each of which is expressed as,

$$U_E \approx \varepsilon_a^2 E_m^* t_m R_a (\pi - \theta_a) + \varepsilon_i^2 E_m^* t_m a_a, \tag{11}$$

$$U_S = -2 a_a W_0, \tag{12}$$

and

$$U_P = -\int \Delta P dV = -\int_{V_i}^{V_a} \left(\frac{K}{V} - P_0\right) dV \approx 2\Delta P_i V_i \left(\frac{\theta_a^3}{3\pi} - \frac{\delta R_a}{R_i}\right). \tag{13}$$

Substituting Eqs. (8)–(10) into Eqs. (11)–(13) and noting the relationship of $a_a = R_a \sin\theta_a = R_i (1 + \lambda_i \theta_a^3) \sin\theta_a$ lead to the overall free energy in the self-adhesion stage

$$\begin{aligned} U &= U_E + U_S + U_P \\ &\approx \varepsilon_a^2 E_m^* t_m R_i \cdot (1 + \lambda_i \theta_a^3)(\pi - \theta_a) + \varepsilon_i^2 E_m^* t_m R_i \cdot (1 + \lambda_i \theta_a^3) \sin\theta_a \\ &\quad - 2R_i W_0 (1 + \lambda_i \theta_a^3) \sin\theta_a + \frac{2}{3} \Delta P_i R_i^2 (1 - 3\pi\lambda_i) \theta_a^3. \end{aligned} \tag{14}$$

The equilibrium condition of the system $\frac{dU}{d\theta_a} = 0$ results in the governing equation of the contact central angle θ_a

$$\begin{aligned} &E_m^* t_m \Big[2 \tfrac{d\varepsilon_a}{d\theta_a} \varepsilon_a (1 + \lambda_i \theta_a^3)(\pi - \theta_a) + \varepsilon_a^2 (3\pi\lambda_i \theta_a^2 - 4\lambda_i \theta_a^3 - 1) \\ &\quad + \varepsilon_i^2 (1 + \lambda_i \theta_a^3) \cos\theta_a + 3\varepsilon_i^2 \lambda_i \theta_a^2 \sin\theta_a \Big] \\ &\quad - 2W_0 \left[3\lambda_i \theta_a^2 \sin\theta_a + (1 + \lambda_i \theta_a^3) \cos\theta_a\right] + 2\Delta P_i R_i (1 - 3\pi\lambda_i) \theta_a^2 = 0, \end{aligned} \tag{15-a}$$

which can be further written as

$$\begin{aligned} &\tilde{E}_m^* \tilde{t}_m \Big[2 \tfrac{d\varepsilon_a}{d\theta_a} \varepsilon_a (1 + \lambda_i \theta_a^3)(\pi - \theta_a) + \varepsilon_a^2 (3\pi\lambda_i \theta_a^2 - 4\lambda_i \theta_a^3 - 1) \\ &\quad + \varepsilon_i^2 (1 + \lambda_i \theta_a^3) \cos\theta_a + 3\varepsilon_i^2 \lambda_i \theta_a^2 \sin\theta_a \Big] \\ &\quad - 2\tilde{W}_0 \left[3\lambda_i \theta_a^2 \sin\theta_a + (1 + \lambda_i \theta_a^3) \cos\theta_a\right] + 2\Delta\tilde{P}_i \tilde{R}_i (1 - 3\pi\lambda_i) \theta_a^2 = 0, \end{aligned} \tag{15-b}$$

with independent dimensionless parameters $\tilde{E}_m^* \tilde{t}_m = \frac{E_m^* t_m}{E_s^* t_s}$, $\tilde{W}_0 = \frac{W_0}{E_s^* t_s}$, $\tilde{P}_i = \frac{P_i \rho}{E_s^* t_s}$, $\tilde{P}_0 = \frac{P_0 \rho}{E_s^* t_s}$ and some other derived ones $\tilde{R}_i = \frac{R_i}{\rho} = \frac{\tilde{E}_m^* \tilde{t}_m}{\tilde{E}_m^* \tilde{t}_m - \Delta\tilde{P}_i}$, $\Delta\tilde{P}_i = \tilde{P}_i - \tilde{P}_0$, $\lambda_i = \frac{2\tilde{R}_i \tilde{P}_i}{3\pi(\tilde{E}_m^* \tilde{t}_m + 2\tilde{R}_i \tilde{P}_i)}$, $\varepsilon_i = \tilde{R}_i - 1$, $\varepsilon_a = (1 + \lambda_i \theta_a^3)\tilde{R}_i - 1$ and $\frac{d\varepsilon_a}{d\theta_a} = 3\lambda_i \theta_a^2 \tilde{R}_i$.

With given parameters, the width of self-adhesion of an elastic membrane adhering on a stress-free substrate can be calculated from Eq. (15).

In the last stage. After self-adhesion of the elastic membrane on the elastic substrate, an externally tensile force F is added on the substrate, which induces variations of the contact width, the contact central angle as well as the tensile strain of the membrane as shown in Fig. 2. Comparing with the initial two stages, the radius increment, the internal gas volume and the tensile strain of the membrane in this stage can be obtained as

$$\delta R_F \approx \frac{2R_i^2 P_i \theta_F^3}{3\pi (E_m^* t_m + 2R_i P_i)} \equiv \lambda_i R_i \theta_F^3, \tag{16}$$

$$V_F \approx \pi R_F^2 \left(1 - \frac{2\theta_F^3}{3\pi}\right) \approx V_i \left(1 + \frac{2\delta R_F}{R_i}\right)\left(1 - \frac{2\theta_F^3}{3\pi}\right), \tag{17}$$

$$R_F = R_i + \delta R_F \approx (1 + \lambda_i \theta_F^3) R_i, \tag{18}$$

$$\varepsilon_F = \frac{R_F - \rho}{\rho} \approx \frac{(1 + \lambda_i \theta_F^3) R_i - \rho}{\rho}. \tag{19}$$

The free energy of the whole system U in the last stage consists of the potential energy U_M associated with the external force F, the elastic strain energies U_E^s and U_E^m stored in the substrate and the

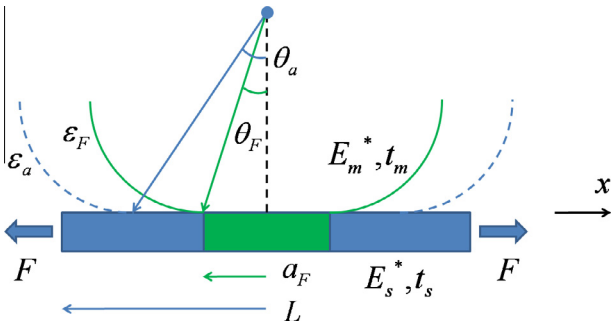

Fig. 2. Schematic of the deformation process from the self-adhesion stage to the one with an external loading on the substrate.

membrane, respectively, the interface adhesion energy U_S as well as the internal energy U_P induced by the compressive gas within the membrane, each of which will be given subsequently.

The tensile displacement induced by the external force F at two ends of the substrate is,

$$u_R = -u_L = \frac{F}{E_s^* t_s}(L - a_F) + \frac{F}{E_s^* t_s + E_m^* t_m} a_F, \tag{20}$$

in which a_F is half of the contact width.

Then, the mechanical potential energy U_M can be written as

$$U_M = -F\left[\frac{F}{E_s^* t_s}(L - a_F) + \frac{F}{E_s^* t_s + E_m^* t_m} a_F\right]. \tag{21}$$

The elastic strain energy stored in the substrate is

$$U_E^s = F^2\left[\frac{(L - a_F)}{E_s^* t_s} + \frac{E_s^* t_s a_F}{(E_s^* t_s + E_m^* t_m)^2}\right]. \tag{22}$$

Due to the assumption of perfect interface adhesion between the membrane and the substrate, the elastic strain in the membrane at the contact region is a superposition of the strain of the membrane itself and the tensile strain of the substrate at the contact region, i.e., $\varepsilon_i + \frac{F}{E_s^* t_s + E_m^* t_m}$. The strain of the membrane outside the contact region is denoted as ε_F. Then, the elastic strain energy stored in the membrane is

$$U_E^m = E_m^* t_m\left[\left(\frac{F}{E_s^* t_s + E_m^* t_m} + \varepsilon_i\right)^2 a_F + \varepsilon_F^2(\pi - \theta_F) R_F\right]. \tag{23}$$

The interface adhesion energy U_S and the internal energy U_P induced by the compressive gas within the membrane at this stage can be expressed as

$$U_S = -2a_F W_0, \tag{24}$$

and

$$U_P = -\int \Delta P dV = -\int_{V_i}^{V_F}\left(\frac{K}{V} - P_0\right) dV \approx 2\Delta P_i V_i\left(\frac{\theta_F^3}{3\pi} - \frac{\delta R_F}{R_i}\right). \tag{25}$$

Thus, the free energy of the whole system U in the last stage is

$$U = U_M + U_E^s + U_E^m + U_S + U_P. \tag{26}$$

The equilibrium condition of the system $\frac{dU}{d\theta_F} = 0$ leads to the governing equation of the contact central angle θ_F as a function of the external loading F,

$$\begin{aligned}&\left[E_m^* t_m\left(\frac{F}{E_s^* t_s + E_m^* t_m} + \varepsilon_i\right)^2 - \frac{E_m^* t_m F^2}{(E_s^* t_s + E_m^* t_m)^2} - 2W_0\right]\\ &\times\left[3\lambda_i\theta_F^2 \sin\theta_F + (1 + \lambda_i\theta_F^3)\cos\theta_F\right] + 2R_i\Delta P_i(1 - 3\pi\lambda_i)\theta_F^2\\ &+ E_m^* t_m \varepsilon_F\left[2(\pi - \theta_F + \pi\lambda_i\theta_F^3 - \lambda_i\theta_F^4)\frac{d\varepsilon_F}{d\theta_F} + (3\pi\lambda_i\theta_F^2 - 4\lambda_i\theta_F^3 - 1)\varepsilon_F\right] = 0,\end{aligned} \tag{27}$$

which can be further written as

$$\begin{aligned}&\left[\tilde{E}_m^* \tilde{t}_m\left(\frac{\tilde{F}}{1 + \tilde{E}_m^* \tilde{t}_m} + \varepsilon_i\right)^2 - \frac{\tilde{E}_m^* \tilde{t}_m \tilde{F}^2}{(1 + \tilde{E}_m^* \tilde{t}_m)^2} - 2\tilde{W}_0\right]\\ &\times\left[3\lambda_i\theta_F^2 \sin\theta_F + (1 + \lambda_i\theta_F^3)\cos\theta_F\right] + 2\tilde{R}_i\Delta\tilde{P}_i(1 - 3\pi\lambda_i)\theta_F^2\\ &+ \tilde{E}_m^* \tilde{t}_m \varepsilon_F\left[2(\pi - \theta_F + \pi\lambda_i\theta_F^3 - \lambda_i\theta_F^4)\frac{d\varepsilon_F}{d\theta_F} + (3\pi\lambda_i\theta_F^2 - 4\lambda_i\theta_F^3 - 1)\varepsilon_F\right] = 0,\end{aligned} \tag{28}$$

with independent dimensionless parameters $\tilde{F} = \frac{F}{E_s^* t_s} = \varepsilon_g$, $\tilde{E}_m^* \tilde{t}_m = \frac{E_m^* t_m}{E_s^* t_s}$, $\tilde{W}_0 = \frac{W_0}{E_s^* t_s}$, $\tilde{P}_i = \frac{P_i \rho}{E_s^* t_s}$, $\tilde{P}_0 = \frac{P_0 \rho}{E_s^* t_s}$ and some other derived dimensionless ones $\tilde{R}_i = \frac{\tilde{E}_m^* \tilde{t}_m}{\tilde{E}_m^* \tilde{t}_m - \Delta\tilde{P}_i}$, $\Delta\tilde{P}_i = \tilde{P}_i - \tilde{P}_0$, $\lambda_i = \frac{2\tilde{R}_i\tilde{P}_i}{3\pi(\tilde{E}_m^* \tilde{t}_m + 2\tilde{R}_i\tilde{P}_i)}$, $\varepsilon_i = \tilde{R}_i - 1$, $\varepsilon_F = (1 + \lambda_i\theta_F^3)\tilde{R}_i - 1$, $\frac{d\varepsilon_F}{d\theta_F} = 3\lambda_i\theta_F^2\tilde{R}_i$.

Eq. (28) can be reduced to Eq. (15) if the external loading F vanishes.

3. Results and discussion

As the two-dimensionally gas-filled membrane adhering on an elastic substrate due to self-adhesion, the central angle θ_a as a function of the interface work of adhesion $\tilde{W}_0$ in Eq. (15) is calculated and shown in Fig. 3 with dimensionless parameters $\tilde{E}_m^* \tilde{t}_m = E_m^* t_m/(E_s^* t_s) = 0.01$, $\tilde{P}_0 = P_0\rho/(E_s^* t_s) = 1$ and $\tilde{P}_i = P_i\rho/(E_s^* t_s) = 1.005$. It is interesting to find that the scaling relation between the central angle and the work of adhesion is nearly $\tilde{W}_0 \sim \theta_a^2$. Furthermore, for a small contact central angle θ_a, the contact half width a_a is approximately proportional to θ_F, i.e. $a_a \sim \theta_a$. Therefore, the scaling law between the contact width and the work of adhesion should nearly be $\tilde{W}_0 \sim a_a^2$, which is consistent well with the scaling relation in a three-dimensionally spherical membrane model (Shanahan, 1997), but different from that in the classically two- or three-dimensional JKR ones, $\tilde{W}_0 \sim a_a^3$ (Barquins, 1988; Johnson et al., 1971); The reason of different scaling laws, as discussed in (Shanahan, 1997), may be that adhesion is "battling" against a volume of solid ($\sim a_a^3$) in a JKR system, while the resistance trying to separate a membrane from a substrate is essentially a surface phenomenon.

After an external force is added to stretch the substrate, the free energy of the whole system is changed, leading to an updated equilibrium state with a reborn contact central angle as given in Eq. (28). The relation between the contact central angle θ_F and the global substrate strain ε_g is shown in Fig. 4, where the work of adhesion is taken as $\tilde{W}_0 = 0.0002$ and the other parameters are same as the second stage, i.e., $\tilde{E}_m \tilde{t}_m = 0.01$, $\tilde{P}_0 = 1$ and $\tilde{P}_i = 1.005$. As shown in Fig. 4, with the global substrate strain increasing, three regimes can be found and are divided by two threshold strains: (i) when the global substrate strain is below the first threshold level, the contact central angle almost keeps unchanged; (ii) after the first threshold level, the contact central angle decreases very quickly with an increasing substrate strain; (iii) when the global substrate strain exceeds the second threshold level, the contact central angle almost equals zero. All the phenomena are very similar to the findings in the experiment of cells cultured on a cyclically

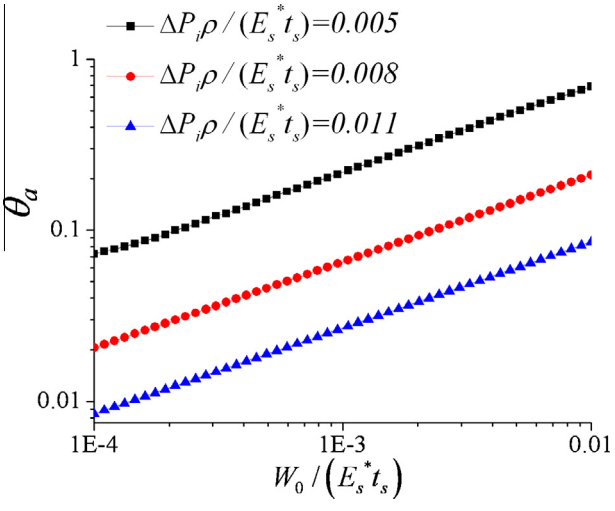

Fig. 3. The relation between the contact central angle θ_a and the interface work of adhesion $\tilde{W}_0$ in the self-adhesion stage with different internal pressures.

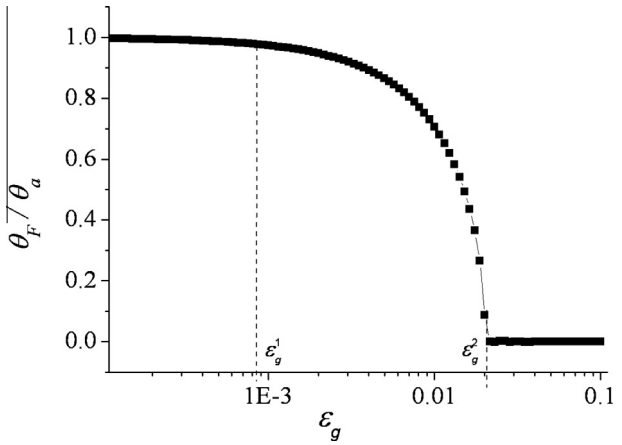

Fig. 4. The relation between the contact central angle θ_a and global substrate strain ε_g in the third stage, in which two threshold strains are denoted as ε_g^1 and ε_g^2.

stretch substrate, where cell reorientation is controlled by two threshold stretch amplitudes (Dartsch and Hammerle, 1986; Neidlingerwilke et al., 1994; Wang et al., 1995), and are consistent well with the results of an earlier model of an elastic cylinder adhering on a stretched substrate (Chen and Gao, 2006b).

In order to analyze the influence factor of the two threshold levels, Fig. 5 gives the contact central angle θ_F as a function of the global substrate strain ε_g with different internal pressures ΔP_i, membrane tensile stiffness $E_m^* t_m$ and interface works of adhesion W_0 in Fig. 5(a)–(c), respectively. It is found that both of the threshold levels decrease with an increasing internal pressure as shown in Fig. 5(a), while they will decrease with a decreasing membrane tensile stiffness or a decreasing interface work of adhesion as shown in Fig. 5(b) and (c), respectively. Since several parameters would show significant influences on the two threshold values and some elastic parameters of cells are not known, it is difficult for us to compare the threshold strains predicted theoretically with those found in a real cell reorientation experiment. However, the behaviors of the contact area predicted by the present model show several features which appear to be qualitatively similar to that of cells cultured on a cyclically stretched substrate. Experiments on cell reorientation in response to cyclic substrate strain also show three characteristic regimes with two threshold strain amplitudes (Dartsch and Hammerle, 1986; Neidlingerwilke et al., 1994; Wang et al., 1995). It was found that cells do not respond to strain amplitudes smaller than 1–2% (Dartsch and Hammerle, 1986). Once the first threshold is reached, an increasing number of cells begin to response to substrate stretch by reorientating themselves away from the stretch direction. meanwhile, the contact width in the direction of stretch decreases. When the strain amplitude is beyond a second threshold level around 5–6%, almost all cells reorient away from the stretch direction (Neidlingerwilke et al., 1994). All these features appear to be in good agreement with our analysis.

As a special case, if the tensile stiffness of substrates $E_s^* t_s$ approaches to infinite (a rigid body), the substrate strain vanishes. The above membrane cannot sense any strain in the substrate, which will achieve an adhesion area equaling to that in the self-adhesion stage.

All the above results show that a homogeneous strain field in substrates could reduce the contact area of an elastic membrane adhering on an elastic substrate, which subsequently leads to the

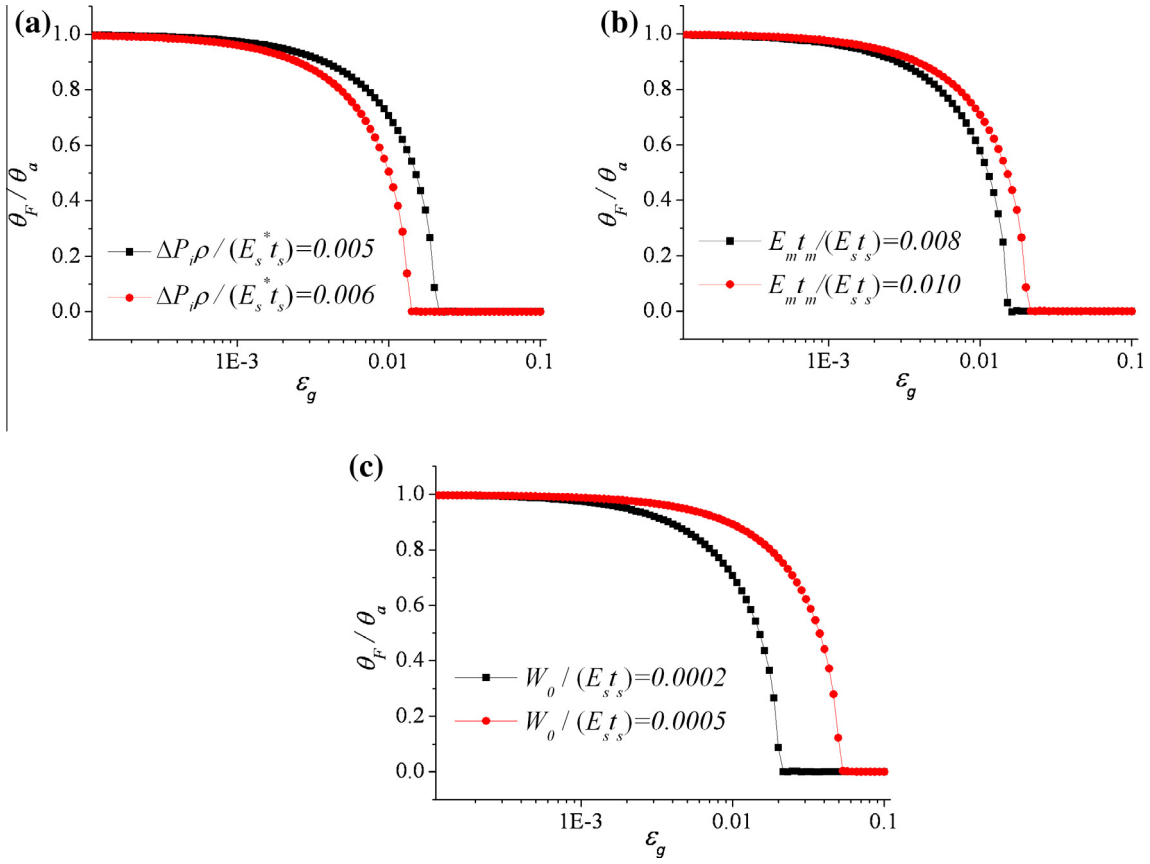

Fig. 5. The contact central angle θ_a as a function of the global substrate strain ε_g in the third stage. (a) For different internal pressures ΔP_i; (b) for different membrane stiffness $E_m^* t_m$; (c) for different interface works of adhesion W_0.

possibility of cell reorientation on the substrate. The larger the homogeneous strain, the smaller the contact area is. However, if the strain field in substrates is inhomogeneous, another interesting phenomenon was found (Chen and Chen, 2014; Chen et al., 2014), i.e., an induced rolling motion of an elastically spherical membrane on an elastic substrate.

4. Conclusions

A two-dimensional contact model of a gas-filled elastic membrane adhesively contacting on a stretched substrate is established in this paper. The whole contact process consists of three stages, including a self-inflated stage, membrane deformation induced by free-adhesion and equilibrium on a stretched substrate. Energy method is adopted in order to find the relation between the contact width described by a central angle and the global substrate strain added on the substrate, considering the effect of internal gas pressure, the elastic stiffness of membrane as well as interface work of adhesion. Two threshold strains exerted on substrates are found which could divide the whole adhesive process into three distinct regimes. All the results share a number of common features with the experimental observation of cell orientation on a stretched substrate. The findings should be helpful for further understanding of adhesion mediated deformation sensing mechanism by which cells or biomolecules may detect mechanical signals in their environments and the design of adhesion mediated deformation sensors.

Acknowledgments

The work reported here is supported by NSFC through Grants #11125211, #11372317 and the 973 Nano-project (2012CB937500).

References

Alberts, B., Bray, D., Lewis, J., Raff, M., Roberts, K., Watson, J.D., 1994. Molecular Biology of the Cell, third ed. Garland, New York, pp. 949–1010.
Bao, G., Suresh, S., 2003. Cell and molecular mechanics of biological materials. Nat. Mater. 2, 715–725.
Barquins, M., 1988. Adherence and rolling kinetics of a rigid cylinder in contact with a natural-rubber surface. J. Adhesion 26, 1–12.
Bell, G.I., 1978. Models for specific adhesion of cells to cells. Science 200, 618–627.
Bischofs, I.B., Schwarz, U.S., 2003. Cell organization in soft media due to active mechanosensing. Proc. Natl. Acad. Sci. U.S.A. 100, 9274–9279.
Buck, R.C., 1980. Reorientation response of cells to repeated stretch and recoil of the substratum. Exp. Cell Res. 127, 470–474.
Chen, L., Chen, S.H., 2014. Rolling motion of an elastic cylinder induced by elastic strain gradients. J. Appl. Phys. 116, 164701.
Chen, S.H., Gao, H.J., 2006a. Non-slipping adhesive contact between mismatched elastic spheres: a model of adhesion mediated deformation sensor. J. Mech. Phys. Solids 54, 1548–1567.
Chen, S.H., Gao, H.J., 2006b. Non-slipping adhesive contact of an elastic cylinder on stretched substrates. Proc. R. Soc. A – Math. Phys. 462, 211–228.
Chen, L., Chen, S.H., Gao, H.J., 2014. Biomimetic study of rolling transport through smooth muscle contraction. Colloids Surf. B 123, 49–52.
Choquet, D., Felsenfeld, D.P., Sheetz, M.P., 1997. Extracellular matrix rigidity causes strengthening of integrin–cytoskeleton linkages. Cell 88, 39–48.
Dartsch, P.C., Hammerle, H., 1986. Orientation response of arterial smooth-muscle cells to mechanical stimulation. Eur. J. Cell Biol. 41, 339–346.
Galbraith, C.G., Sheetz, M.P., 1998. Forces on adhesive contacts affect cell function. Curr. Opin. Cell Biol. 10, 566–571.
Gao, H.J., Shi, W.D., Freund, L.B., 2005. Mechanics of receptor-mediated endocytosis. Proc. Natl. Acad. Sci. U.S.A. 102, 9469–9474.
Gao, H.J., Qian, J., Chen, B., 2011. Probing mechanical principles of focal contacts in cell-matrix adhesion with a coupled stochastic-elastic modelling framework. J. R. Soc. Interface 8, 1217–1232.
Geiger, B., Bershadsky, A., 2002. Exploring the neighborhood: adhesion-coupled cell mechanosensors. Cell 110, 139–142.
Girard, P.R., Nerem, R.M., 1995. Shear-stress modulates endothelial-cell morphology and F-actin organization through the regulation of focal adhesion-associated proteins. J. Cell. Physiol. 163, 179–193.
Haston, W.S., Shields, J.M., Wilkinson, P.C., 1983. The orientation of fibroblasts and neutrophils on elastic substrata. Exp. Cell Res. 146, 117–126.
Hiramoto, Y., 1963. Mechanical properties of sea urchin eggs. 1. Surface force and elastic modulus of cell membrane. Exp. Cell Res. 32, 59-&.
Huang, S., Ingber, D.E., 1999. The structural and mechanical complexity of cell-growth control. Nat. Cell Biol. 1, E131–E138.
Ingber, D.E., 1993. Cellular tensegrity – Defining new rules of biological design that govern the cytoskeleton. J. Cell Sci. 104, 613–627.
Johnson, K.L., Kendall, K., Roberts, A.D., 1971. Surface energy and contact of elastic solids. Proc. R. Soc. London, Ser.-A 324, 301–313.
Jungbauer, S., Gao, H.J., Spatz, J.P., Kemkemer, R., 2008. Two characteristic regimes in frequency-dependent dynamic reorientation of fibroblasts on cyclically stretched substrates. Biophys. J. 95, 3470–3478.
Kong, D., Ji, B.H., Dai, L.H., 2008. Stability of adhesion clusters and cell reorientation under lateral cyclic tension. Biophys. J. 95, 4034–4044.
Liu, K.K., 2006. Deformation behaviour of soft particles: a review. J. Phys. D Appl. Phys. 39, 189–199.
Liu, K.K., Williams, D.R., Briscoe, B.J., 1996. Compressive deformation of a single microcapsule. Phys. Rev. E 54, 6673–6680.
Lo, C.M., Wang, H.B., Dembo, M., Wang, Y.L., 2000. Cell movement is guided by the rigidity of the substrate. Biophys. J. 79, 144–152.
Lorz, B., Simson, R., Nardi, J., Sackmann, E., 2000. Weakly adhering vesicles in shear flow: tanktreading and anomalous lift force. Europhys. Lett. 51, 468–474.
Lulevich, V.V., Andrienko, D., Vinogradova, O.I., 2004. Elasticity of polyelectrolyte multilayer microcapsules. J. Chem. Phys. 120, 3822–3826.
Moretti, M., Prina-Mello, A., Reid, A.J., Barron, V., Prendergast, P.J., 2004. Endothelial cell alignment on cyclically-stretched silicone surfaces. J. Mater. Sci.-Mater. Med. 15, 1159–1164.
Neidlingerwilke, C., Wilke, H.J., Claes, L., 1994. Cyclic stretching of human osteoblasts affects proliferation and metabolism – A new experimental-method and its application. J. Orthopaed. Res. 12, 70–78.
Qian, J., Gao, H.J., 2010. Soft matrices suppress cooperative behaviors among receptor-ligand bonds in cell adhesion. PLoS ONE 5, 0012342.
Sen, S., Subramanian, S., Discher, D.E., 2005. Indentation and adhesive probing of a cell membrane with AFM: theoretical model and experiments. Biophys. J. 89, 3203–3213.
Shanahan, M.E.R., 1997. A novel test for the appraisal of solid/solid interfacial interactions. J. Adhesion 63, 15–29.
Shanahan, M.E.R., 2003. Adhesion of a liquid-filled spherical membrane. J. Adhesion 79, 881–891.
Wang, N., Butler, J.P., Ingber, D.E., 1993. Mechanotransduction across the cell-surface and through the cytoskeleton. Science 260, 1124–1127.
Wang, H.C., Ip, W., Boissy, R., Grood, E.S., 1995. Cell orientation response to cyclically deformed substrates: experimental validation of a cell model. J. Biomech. 28, 1543–1552.
Wong, J.Y., Velasco, A., Rajagopalan, P., Pham, Q., 2003. Directed movement of vascular smooth muscle cells on gradient-compliant hydrogels. Langmuir 19, 1908–1913.
Xu, D.W., Liechti, K.M., 2011. Analytical and experimental study of a circular membrane in adhesive contact with a rigid substrate. Int. J. Solids Struct. 48, 2965–2976.
Zhang, W.L., Qian, J., Yao, H.M., Chen, W.Q., Gao, H.J., 2012. Effects of functionally graded materials on dynamics of molecular bond clusters. Sci. China Phys. Mech. 55, 980–988.
Zhang, W.L., Lin, Y., Qian, J., Chen, W.Q., Gao, H.J., 2013. Tuning molecular adhesion via material anisotropy. Adv. Funct. Mater. 23, 4729–4738.